(12) INTERNATIONAL APPLICATION PUBLISHED UNDER THE PATENT COOPERATION TREATY (PCT)

(19) World Intellectual Property Organization
International Bureau

(43) International Publication Date
23 March 2023 (23.03.2023)

WIPO | PCT

(10) International Publication Number
WO 2023/044121 A1

(51) International Patent Classification:
E04C 5/00 (2006.01) *B32B 13/04* (2006.01)
B28B 23/00 (2006.01) *C04B 7/02* (2006.01)

(21) International Application Number:
PCT/US2022/044016

(22) International Filing Date:
19 September 2022 (19.09.2022)

(25) Filing Language: English

(26) Publication Language: English

(30) Priority Data:
63/245,300 17 September 2021 (17.09.2021) US

(71) Applicant: **UNIVERSITY OF PITTSBURGH - OF THE COMMONWEALTH SYSTEM OF HIGHER EDUCATION** [US/US]; 1st Floor Gardner Steel Conference Center (GSCC), 130 Thackeray Avenue, Pittsburgh, PA 15260 (US).

(72) Inventors: **ALAVI, Amir**; 849 Northridge Drive, Pittsburgh, PA 15216 (US). **BARRI, Kaveh**; 3429 Dawson Street, Pittsburgh, PA 15213 (US). **KHAZANOVICH, Lev**; 210 Cypress Knoll Drive, Sewickley, PA 15143 (US). **KLINE, Jake**; 67 Lakeside Trail, Kinnelon, NJ 07405 (US). **ZHANG, Qianyun**; 7119 Card Lane, Pittsburgh, PA 15208 (US).

(74) Agent: **BANGOR, Paul D., Jr**; Clark Hill PLC, 301 Grant Street, 14th Floor, Pittsburgh, PA 15219 (US).

(81) Designated States *(unless otherwise indicated, for every kind of national protection available)*: AE, AG, AL, AM, AO, AT, AU, AZ, BA, BB, BG, BH, BN, BR, BW, BY, BZ, CA, CH, CL, CN, CO, CR, CU, CV, CZ, DE, DJ, DK, DM, DO, DZ, EC, EE, EG, ES, FI, GB, GD, GE, GH, GM, GT, HN, HR, HU, ID, IL, IN, IQ, IR, IS, IT, JM, JO, JP, KE, KG, KH, KN, KP, KR, KW, KZ, LA, LC, LK, LR, LS, LU, LY, MA, MD, ME, MG, MK, MN, MW, MX, MY, MZ, NA, NG, NI, NO, NZ, OM, PA, PE, PG, PH, PL, PT, QA, RO, RS, RU, RW, SA, SC, SD, SE, SG, SK, SL, ST, SV, SY, TH, TJ, TM, TN, TR, TT, TZ, UA, UG, US, UZ, VC, VN, WS, ZA, ZM, ZW.

(84) Designated States *(unless otherwise indicated, for every kind of regional protection available)*: ARIPO (BW, GH, GM, KE, LR, LS, MW, MZ, NA, RW, SD, SL, ST, SZ, TZ, UG, ZM, ZW), Eurasian (AM, AZ, BY, KG, KZ, RU, TJ, TM), European (AL, AT, BE, BG, CH, CY, CZ, DE, DK, EE, ES, FI, FR, GB, GR, HR, HU, IE, IS, IT, LT, LU, LV, MC, MK, MT, NL, NO, PL, PT, RO, RS, SE, SI, SK, SM, TR), OAPI (BF, BJ, CF, CG, CI, CM, GA, GN, GQ, GW, KM, ML, MR, NE, SN, TD, TG).

Published:
— *with international search report (Art. 21(3))*
— *before the expiration of the time limit for amending the claims and to be republished in the event of receipt of amendments (Rule 48.2(h))*

WO 2023/044121 A1

(54) Title: SUPER-COMPRESSIBLE METAMATERIAL CONCRETE AND METHOD FOR MAKING SAME

(57) Abstract: A metamaterial, comprising: an auxetic lattice structure with snap-through buckling behavior comprising a plurality of rows; wherein the lattice defines a holey arrangement array; and cement, concrete or any other brittle materials disposed in the auxetic lattice structure.

SUPER-COMPRESSIBLE METAMATERIAL CONCRETE AND METHOD FOR MAKING SAME

RELATED APPLICATION

[0001] This application claims priority benefit under 35 U.S.C. § 119(e) of U.S. Provisional Application No. 63/245,300 filed September 17, 2021 the contents of which are herein incorporated by reference.

FIELD OF THE DISCLOSURE

Technical field

[0002] The present disclosure generally relates to the field of mechanical metamaterials, concrete and cementitious material fabrication methods.

Background

[0003] The present disclosure presents a new class of lightweight reinforced composite concrete materials with unprecedented compressibility and mechanical tunability. The present disclosure presents the striking concept of "metamaterial concrete" by harnessing the power of metamaterial systems to fabricate self-recovering concrete structures. The preferred metamaterial concrete systems of the present disclosure comprise reinforcement auxetic polymer lattices with snap-through buckling behavior fully embedded inside a concrete matrix. Preferred concrete metamaterials have been built with different geometries and reinforcement levels. Experimental and numerical studies have been conducted to investigate the mechanical properties of the preferred concrete metamaterials of the present disclosure, which highlight the potential of such preferred concrete metamaterials to transform the current design practice in concrete industry.

[0004] Concrete is the most utilized material in the construction industry. It is eyed favorably in construction due to fast-developing compressive strength, easiness to shape, and low cost to weight ratio. Those very same advantages of concrete are matched with some serious long-term issues in its post-construction lifetime. Concrete performs poorly in tension to the magnitude that it performs well in compression. Its extreme brittleness increases vulnerability to weathering and fatigue effects. Massive amounts of time and research have been dedicated to improving concrete properties by changing either the mixture recipe or the reinforcement method [1-5]. The commonality between these studies is to fundamentally change concrete behavior to increase ductility. A ductile material can deform plasticly upon yielding and maintain functionality, whereas a brittle material such as concrete will fail immediately at yield. Ductility can increase the concrete materials capacity in any loading condition, most importantly bending, compression, and tension for structural applications. Changing mixture properties has shown to be effective in increasing compressibility [1], whereas reinforcement bolsters flexural capacity [3]. However, a next technological revolution in this arena is arguably creating a new generation of concrete materials that offer compressibility and mechanical tunability simply via a rational architectural design. This goal can be potentially achieved using the architected mechanical metamaterial concepts. Mechanical metamaterials are artificial material with engineered micro/nano-scale structures to provide unprecedented mechanical properties [6]. There has been a growing interest in exploring various aspects of metamaterials for engineering applications in recent years [7]. While most of the studies in the area of metamaterial are focused on designing micro/nano-scale structures [8], a major challenge ahead of the metamaterial science is how to adopt them for large/mega scale applications, in particular in construction industry.

[0005] According to the present disclosure, the concept of "metamaterial concrete" will comprise a new class of lightweight reinforced composite concrete materials with dramatic compressibility and mechanical tunability. To this aim, the present disclosure introduces preferred mechanical metamaterial design approaches into the fabrication of concrete structures. In preferred concrete metamaterials of the present disclosure, auxetic polymer lattices embedded inside the concrete matrix serve as reinforcement elements. The present disclosure further encompasses preferred self-recovering snapping concrete metamaterials and describes preferred material geometries, concrete mixture proportions, and testing results. Potential groundbreaking

applications of preferred concrete metamaterials of the present disclosure are described to further accentuate the full capabilities of such concrete metamaterials in commercial construction.

BRIEF SUMMARY OF THE DISCLOSURE

[0006] In a preferred aspect, the present disclosure comprises a metamaterial, comprising: an auxetic lattice structure with snap-through buckling behavior comprising a plurality of rows; wherein the lattice defines a holey arrangement array; and cement, concrete or any other brittle materials disposed in the auxetic lattice structure.

[0007] In another preferred aspect of a metamaterial of the present disclosure, the auxetic lattice structure comprises a polymer.

[0008] In a further preferred aspect of a metamaterial of the present disclosure, the auxetic lattice structure comprises a thermoplastic polyurethane.

[0009] In another preferred aspect of a metamaterial of the present disclosure, each row of the auxetic lattice structure defines a channel or conduit in which the cement, concrete or any other brittle materials are disposed.

[00010] In an additional preferred aspect of a metamaterial of the present disclosure, each channel or conduit has an open side or end for receiving the cement, concrete or any other brittle materials.

[00011] In another preferred aspect of a metamaterial of the present disclosure, each row defines one or more curved sections.

[00012] In yet another preferred aspect of a metamaterial of the present disclosure, the each row defines a plurality of curved sections.

[00013] In another preferred aspect of a metamaterial of the present disclosure, the cement or concrete comprises a mixture of Type I/II Portland cement and water.

[00014] In yet another preferred aspect of a metamaterial of the present disclosure, a maximum water to cement ratio of 0.45.

[00015] In another preferred aspect of a metamaterial of the present disclosure, the compressibility of the metamaterial is varied by varying the Young's Modulus and/or Poisson's Ratio of the auxetic lattice structure and/or the cement or concrete.

[00016] In a further preferred aspect of a metamaterial of the present disclosure, the metamaterial does not exhibit transverse strain under compression.

[00017] In another preferred aspect of a metamaterial of the present disclosure, the holey arrangement array comprises a 3x3 array or a 5x5 array.

[00018] In yet a further preferred aspect, a metamaterial of the present disclosure further comprises one or more level or planar surfaces.

[00019] In another preferred aspect of a metamaterial of the present disclosure, the metamaterial undergoes pattern transformation under compression to allow vertical displacement of the metamaterial, equivalent to a dimension of the holey arrangement array, from a default position and when compression of the metamaterial is discontinued, the metamaterial undergoes another pattern transformation and returns to the default position.

[00020] In a further preferred aspect of a metamaterial of the present disclosure, the auxetic lattice structure comprises a material with a low Young's modulus (E) and high Poisson's ratio (ν).

[00021] In another preferred aspect, the present disclosure comprises a metamaterial, comprising: a flex design comprising a concrete or cement material disposed in an auxetic structure with snap-through buckling behavior; and a cement, concrete or any other brittle materials disposed in the auxetic lattice structure.

[00022] In another preferred aspect of a metamaterial of the present disclosure, the auxetic structure has a plurality of rows and defines a holey arrangement array.

[00023] In yet another preferred aspect of a metamaterial of the present disclosure, the auxetic structure comprises a polymer or a thermoplastic polyurethane.

[00024] In a further preferred aspect of a metamaterial of the present disclosure, each row of the auxetic structure defines a channel or conduit in which the cement, concrete or any other brittle materials are disposed.

[00025] In another preferred aspect of a metamaterial of the present disclosure, each row defines one or more curved sections.

[00026] In an additional preferred aspect of a metamaterial of the present disclosure, the cement or concrete comprises a mixture of Type I/II Portland cement and water.

[00027] In yet another preferred aspect of a metamaterial of the present disclosure, the a maximum water to cement ratio of 0.45.

[00028] In another preferred aspect of a metamaterial of the present disclosure, the compressibility of the metamaterial is varied by varying the Young's Modulus and/or Poisson's Ratio of the auxetic lattice structure and/or the cement or concrete.

[00029] In yet another preferred aspect of a metamaterial of the present disclosure, the metamaterial does not exhibit transverse strain under compression.

[00030] In another preferred aspect of a metamaterial of the present disclosure, the holey arrangement array comprises a 3x3 array or a 5x5 array.

[00031] In yet a further preferred aspect, a metamaterial of the present disclosure further comprises one or more level or planar surfaces.

[00032] In another preferred aspect of a metamaterial of the present disclosure, the metamaterial undergoes pattern transformation under compression to allow vertical displacement of the metamaterial, equivalent to a dimension of the holey arrangement array, from a default position and when compression of the metamaterial is discontinued, the metamaterial undergoes another pattern transformation and returns to the default position.

[00033] In yet another preferred aspect of a metamaterial of the present disclosure, the auxetic structure comprises a material with a low Young's modulus (E) and high Poisson's ratio (v).

BRIEF DESCRIPTION OF THE DRAWINGS

[00034] For the present disclosure to be easily understood and readily practiced, the present disclosure will now be described for purposes of illustration and not limitation in connection with the following figures, wherein:

[00035] **FIG. 1** shows a preferred composite metamaterial concrete system with self-recovering snapping segments of the present disclosure.

[00036] **FIG. 2** shows an example of a unit of material under compression exhibiting positive Poisson's ratio (top) and negative Poisson's ratio (bottom).

[00037] **FIG. 3.** shows preferred metamaterial concrete polymeric lattices of the present disclosure comprised of (a) 3×3 unit cells and (b) 5×5 unit cells.

[00038] **FIG. 4.** shows preferred fabricated metamaterial concrete polymeric lattices of the present disclosure comprised of (a) 3×3 unit cells, (b) 5×5 unit cells.

[00039] **FIG. 5.** shows the results of stiffness versus time for tests at Stage 1 compression for a preferred concrete metamaterial of the present disclosure at: (a) 4 mm vertical displacement, (b) 5 mm vertical displacement.

[00040] **FIG. 6.** shows P-δ curves illustrated for preferred concrete metamaterials of the present disclosure comprising: (a) a 3×3 unit cell concrete metamaterial **10A** and (b) a 5×5 unit cell concrete metamaterial **10B**.

[00041] **FIG. 7.** shows cyclic compression strain readings plotted against time for preferred concrete metamaterials of the present disclosure comprising: (a) a 3×3 unit cell concrete metamaterial **10A** measured with a side gauge, (b) a 3×3 unit cell concrete metamaterial **10A** measured with a center gauge and (c) a 5×5 unit cell concrete metamaterial **10B** measured with a side gauge.

[00042] **FIG. 8.** shows ultimate compression strain readings plotted against time for preferred concrete metamaterials of the present disclosure comprising: (a) 3×3 unit cell concrete metamaterial **10A** measured with a side gauge and (b) 3×3 unit cell concrete metamaterial **10A** measured with a center gauge.

[00043] **FIG. 9.** shows FE simulation results comprising: (a) Mises stresses, (b) Transverse strains, (c) Longitudinal strains for a preferred concrete metamaterial of the present disclosure comprising a 3×3 unit cell concrete metamaterial.

[00044] **FIG. 10.** shows illustrations of damage progression through a cycle of compression for preferred concrete metamaterials of the present disclosure comprising: (a) a 3×3 unit cell concrete metamaterial **10A** and (b) a 5×5 concrete metamaterial **10B**.

[00045] **FIG. 11.** shows a preferred unit slab concept design for the 3×3 metamaterial polymer formwork of the present disclosure with potential applications of the proposed metamaterial concrete: (a) a high energy absorbing engineered materials arresting system, (b) metamaterial concrete base isolation system, (c) A shock absorbent bike lane pavement.

DETAILED DESCRIPTION

Principles of Metamaterial Concrete Systems

[00046] Classifying a metamaterial is not based on material composition. What really defines a metamaterial is the geometrical arrangement of the subunits, which can bestow unthinkable properties such as zero or negative Poisson's ratio, negative stiffness, negative compressibility, and vanishing shear modulus [9,10]. **Figure 1** shows a preferred composite metamaterial concrete system **10** of the present disclosure with tunable buckling, self-recovering, and energy absorption responses. The metamaterial concrete **10** of the present disclosure is naturally a mechanical metamaterial with zero Poisson's ratio because of its auxetic geometry. Mathematically speaking, Poisson's ratio is the negative ratio of lateral strain to longitudinal strain. **Figure 2** shows a schematic representation of the positive and negative Poisson's ratio. A specimen placed under uniform compression in the longitudinal direction normally shrinks longitudinally and expands laterally. Instead of expanding laterally, an auxetic metamaterial with negative Poisson's ratio is designed to shrink laterally under compression [9]. A preferred metamaterial concrete system **10** of the present disclosure with zero Poisson's ratio does not exhibit transverse strain under compression. Preferred concrete metamaterials of the present disclosure achieve this unique feature via introducing the so-called "Flex Design", where conventional concrete materials **14** are cast into an auxetic mechanical metamaterial polymeric structure **12** with snap-through buckling behavior. This hybrid design approach could significantly increase the compressibility of the concrete materials. The compressibility of a rigid body can be defined in engineering terms as the inverse of the body's bulk modulus (K). K is also known as the modulus of volume expansion as it is inherent material resistance to volumetric change. Preferably, the compressibility of a metamaterial concrete **10** of the present disclosure can be fine tuned by interfacing materials with different Young's Moduli and Poisson's Ratio in unique geometries. The design follows principles of symmetry and contains two level surfaces **16, 18** for load bearing purposes.

[00047] The metamaterial concrete **10** of the present disclosure undergoes pattern transformation under compression to allow vertical displacement equivalent to the size of the unit cells. If the force is released, the metamaterial concrete **10** undergoes another pattern transformation and returns to the default position. This compressibility is further improved by the auxetic cells **12** connecting the holey arrangement that comprises an array of holes **20** preferably defined by a plurality of open cylinders **21**. The metamaterial concrete **10** is afforded two degrees of freedom of compressibility where it can volumetrically contract under an applied load and completely recover when the load is released. The most suitable material for the design of the embedded auxetic polymeric structure **12** is preferably a material with a low Young's modulus (E) and high Poisson's ratio (ν). In a preferred metamaterial concrete **10** of the present disclosure, the cement paste mixture provides the required strength and stiffness needed to complete the composite metamaterial **10**. The remaining geometry of the metamaterial concrete **10** of the present disclosure interlinks the auxetic arrangement. Therefore, the concrete provides horizontal and vertical stability, and enhanced compressibility. Here, the embedded auxetic structure **12** also serves as concrete reinforcement and defines channels or conduits **22** for receiving the concrete **14**. The difference in concrete failure modes is completely different when reinforcement is used. An increasingly popular type of concrete reinforcement is fiber reinforced polymer (FRP). FRPs are lighter and more corrosion resistant than steel rebar [11]. The fiber in FRP is typically made of carbon or glass, which is woven into a thin fabric and wrapped around the cylinders after the specimen cure. Exterior reinforcement still provides the increased tension capacity of steel rebar, but also increases the compression efficiency of concrete. The current limitation of the FRP concrete is the bonding between the reinforcement and the concrete. For instance, when steel reinforced concrete experiences large bending forces, the rebar deforms and forms a much stronger bond to the concrete. In the FRP applications, the bonding between the FRP and concrete is not strengthened by applied loading, rather it is the first component to fail in this system [11,12]. The preferred auxetic polymeric structures **12** of the present disclosure takes these shortcomings into consideration and provides a solution that would keep the concrete and polymer reinforcement structures **12** bonded in all possible loading conditions. The geometry of the preferred concrete metamaterials **10** of the present disclosure prevent lateral expansion similar to the FRP reinforcement but also allows for energy dissipation to ensure that neither the polymer structure **12** nor the concrete **14** incur any damage. Preferred concrete metamaterials **10** of the present

disclosure possess a property better known as damping, seen in more and more in seismic applications to reduce vibration fatigue on any structure. Under uniaxial compression, the composite metamaterial concrete **10** of the present disclosure can be compressed significantly and completely recover in a matter of seconds. Even when flaws are present on a surface of the concrete **14**, or a crack progresses in therein, the bonding between the polymer **12** and the concrete **14** is preferably strong enough to maintain the composite metamaterial **10** at full strength.

[00048] In order to validate the preferred concrete metamaterials **10** of the present disclosure, proof-of-concept porotypes were fabricated and tested them under cyclic loadings.

[00049] Most material innovations have a number of extended variables that can lead the designing engineer to the ideal strength and material behaviors. This principle would arguably apply to the preferred concrete metamaterials **10** of the present disclosure. The ideal ratio of polymer to concrete should be sought simultaneously. We created two potential metamaterial concrete designs with different amounts of polymer reinforcement to accomplish this task. The designs for polymeric lattices with self-recovering snapping segments are shown in **Figure 3**. The first preferred concrete metamaterial design **10A** with 3×3 unit cells has a lower ratio of polymer to concrete cement paste compared to the second preferred concrete metamaterial design **10B** with a 5×5 unit cell design. Such ratio of polymer to concrete cement paste of the preferred concrete metamaterial designs **10A** and **10B** potentially affects the compressibility and magnitude of strain in the concrete cement paste thereof. Neither of these preferred concrete metamaterial designs **10A** and **10B** may qualify as the "ideal" material ratio as an ideal design is dependent on the realistic application of the material. For the testing purposes, we decided that cubic dimensions would provide empirical results regarding the longitudinal displacement and the subsequent recovery of the metamaterial when the compression is released. Therefore, the lattices **12** were scaled to 6 in × 6 in× 6 in as a testing standard for future iterations of this design. The auxetic lattices **12** were 3D printed using a Raise 3D Pro2 printer. PolyFlex™ filaments were used to print the samples. PolyFlex™ TPU95 is a thermoplastic polyurethane (TPU) based filament available from Polymaker LLC at www.polymaker.com. In addition to the PolyFlex auxetic lattices **12**, a modular 6 inch cubic base was printed to stabilize the metamaterial designs during the pour phase.

[00050] The concrete portion **14** of the composite concrete metamaterial **10** is preferably cement paste, a basic mixture of Type I/II Portland cement and water. ACI 318-14 Table 19.3.2.1 specifies a maximum water to cement ratio of 0.45 or 45% for plain concrete [13]. This was considered a sufficient starting point for the concrete sections. The pours were executed carefully for each metamaterial design to avoid distorting the geometry of the PolyFlex polymer reinforcement structures **12**, which would conversely affect the overall compressibility of the concrete metamaterial **10**. Each section or row **15** was filled with the concrete **14** in increments of 2 inches and the layer was consolidated with a small metal rod or gentle vibrations to the mold walls using a rubber mallet. When the cement paste reached the top of the mold, the cover was gently cleaned to avoid any binding with the cement paste as the sample cured. The top was covered, and the sample set aside to dry for 24 hours. Once the samples were drying, the modular molds and covers were gently removed, and the samples submerged in water to cure. The samples were cured for 2 weeks, and once finished they were removed from the water and prepared for the testing phase.

[00051] Static testing performance of each design **10A**, **10B** was assessed via the Instron® 8874 Biaxial Servohydraulic Fatigue Testing System. There were two tests implemented to estimate the compressive properties of both metamaterial designs **10A**, **10B**. Both designs **10A**, **10B** were initially tested in cyclic compression, consisting of 10 cycles of compression and subsequent release at a rate of 0.05 Hz. These trials were repeated to increase the vertical displacement of the concrete metamaterial **10A**, **10B** from the default at rest state. Each trial in cyclic compression will be referred to as a stage in this present disclosure. The vertical displacement was deliberately kept small as to not exceed the space allocated by the auxetic cells **12**. Following these tests, the samples were placed under ultimate compression. Ultimate compression featured a one-time vertical displacement exceeding the auxetic cell space to observe how the concrete metamaterials **10A**, **10B** would recover under extreme loading conditions. The compression rate was the same as cyclic compression and once the position was achieved, each concrete metamaterial **10A**, **10B** was held there for 10 seconds and released.

[00052] Another important parameter to analyze while the concrete metamaterials **10A**, **10B** are under compression is the strain in the cement paste layers **14**. It is important to observe the

magnitude and orientation of the strains in the cement layer **14** to analytically prove that each concrete metamaterial **10A**, **10B** only keeps the cement paste **14** engaged in compression. For this purpose, the middle cement layer **19** for each concrete metamaterial **10A**, **10B** was chosen as the focal point for strain analysis. The strain analysis was set to occur at the central cement paste layer **19** of each concrete metamaterial **10A**, **10B**. To observe the relative strains in the cement layer **14**, a strain gauge **30** was placed at approximately 2 in (1/3 of the horizontal distance of the layer) and another at approximately 4 in (2/3 of the horizontal distance of the layer) (**Figure 4**). Aside from comparing the compressibility of each concrete metamaterial **10A**, **10B**, a baseline comparison to concrete was also desired. To illustrate this comparison experimentally, the molds were reused to cast a plain cement paste cube to serve as the control variable in testing. The same water to cement ratio and cure times were implemented to ensure an accurate baseline comparison.

[00053] The 3×3 metamaterial concrete **10A** was tested over two trials in three stages of cyclic compression. The first trial achieved vertical displacements of 5 mm, 8 mm, and 11 mm for Stages 1, 2, and 3, respectively. The second trial achieved vertical displacements of 4 mm, 9 mm, and 12 mm for Stages 1, 2, and 3, respectively. **Table 1** shows the stages of cyclic compression for the 3×3 metamaterial concrete **10A**.

Table 1. Cyclic compression stages for the 3×3 metamaterial concrete **10A**.

3×3 Metamaterial	Cross Sectional Area (mm^2)	Initial Height (mm)	Final Height (mm)	Initial Volume (mm^3)	Final Volume (mm^3)
Stage 1 – Trial 1	22500	150	145.99	3,375,000	3,284,775
Stage 1 – Trial 2			144.99		3,262,267
Stage 2 – Trial 1			141.98		3,194,596
Stage 2 – Trial 2			141.99		3,194,705
Stage 3 – Trial 1			138.98		3,127,120
Stage 3 – Trial 2			137.98		3,104,459

[00054] For the 5×5 metamaterial concrete **10B**, the first trial only made it to one stage of 5 mm vertical displacement due to overconsolidation of cement paste at the bottom layer of the PolyFlex mold. The overconsolidation forced closure of the auxetic cells on one side of the PolyFlex mold preventing proper compression recovery. The second trial produced viable results achieving 2 mm, 4.5 mm, 7 mm, and 9.5 mm for Stages 1, 2, 3, and 4, respectively (**Table 2**).

Table 2. Cyclic compression stages for the 5×5 metamaterial concrete **10B**.

5×5 Metamaterial	Cross Sectional Area (mm^2)	Initial Height (mm)	Final Height (mm)	Initial Volume (mm^3)	Final Volume (mm^3)
Stage 1	22500	150	147.99	3,375,000	3,329,852
Stage 2			145.49		3,273,538
Stage 3			142.99		3,217,188
Stage 4			140.48		3,160,776

[00055] One potential source of error in the positioning that would introduce errors in following calculations is the recovery distance of each concrete metamaterial **10A**, **10B** was not maximized prior to each subsequent stage of compression. It was observed that the Instron would initiate the next cycle before each concrete metamaterial **10A**, **10B** had a chance to fully recover to the initial position. This error was eliminated in the above calculations by only considering the change in position after the beginning of the second cycle. With that in mind, the important properties such as bulk modulus, recovery rate, and stiffness may be slightly higher due to this adjustment. The Instron device also recorded the magnitude of the applied compression load over time. Unlike the position, the applied load took longer to stabilize over 10 cycles of compression. Typically, the load cycles attained consistency after the 5^{th} or 6^{th} cycle of compression. In attempting to stabilize, the Instron would not adequately release each concrete metamaterial **10A**, **10B** and compensated by applying a larger compressive force in the next cycle. This phenomenon was noted, and the unstable data eliminated when considering the maximum load applied to each concrete metamaterial **10A**, **10B** during each cyclic testing stage. Given a uniform cross-sectional area, a maximum change in pressure was calculated for each cyclic stage (Table 3).

Table 3. Maximum loading conditions observed at each stage for each concrete metamaterial **10A**, **10B**.

	Stage	Maximum Force (N)	Max Pressure (MPa)
3×3 Metamaterial	Stage 1 – Trial 1	2798	0.124
	Stage 1 – Trial 2	1088	0.053
	Stage 2 – Trial 1	2934	0.130
	Stage 2 – Trial 2	1160	0.060
	Stage 3 – Trial 1	1392	0.068
	Stage 3 – Trial 2	3205	0.142

5×5 Metamaterial	Stage 1	1091	0.048
	Stage 2	3590	0.160
	Stage 3	5190	0.231
	Stage 4	5787	0.257

Calculating the Bulk Modulus

[00056] K is a materials inherent resistance to volumetric change under an applied pressure. This can be represented by the equation $K = -V\frac{dP}{dV}$, where V is the initial volume, dP is the differential change in pressure, and dV is the differential change in volume. Since the element under consideration is not on a differential scale, this equation can be modified to $K = -V\frac{\Delta P}{\Delta V}$. The volumetric changes in the specimen shown above was calculated from the achieved vertical displacement at each stage of cyclic compression. Coupling that with the maximum applied pressure to achieve the desired displacement, all of knowns are present to approximate the bulk modulus for each stage. **Table 4** shows the averaged outcomes to make accumulative approximation of the bulk modulus of each concrete metamaterial **10A**, **10B**.

Table 4- Bulk moduli calculated at each stage each concrete metamaterial **10A**, **10B**.

3×3 Metamaterial	*K* (MPa)	*5×5 Metamaterial*	*K* (MPa)
Stage 1 – Trial 1	4.65	Stage 1	3.62
Stage 1 – Trial 2	1.57	Stage 2	5 31
Stage 2 – Trial 1	2 44	Stage 3	4.93
Stage 2 – Trial 2	1.13	Stage 4	4 05
Stage 3 – Trial 1	0.93	Mean	4.48
Stage 3 – Trial 2	1.78	-	-
Mean	1.57	Mean	4 48

[00057] It was inferred that the 3×3 concrete metamaterial **10A** would exhibit higher compressibility due to the larger space afforded by the auxetic cells. Conceptually speaking, these larger gaps of free space would permit larger compression and recovery without significant damage to the concrete layers. As indicated by the data, this thought process holds true as the mean bulk modulus of the 3×3 concrete metamaterial **10A** is approximately 3 times less than the 5×5 each concrete metamaterial **10B**. Based on this trend, it would be desirable to direct future work towards designing different arrangements to devise a way to fine tune bulk modulus. A definitive

proportion cannot be established at this point, but a trend has at least been revealed on how to control this material property in design. Overall, each of the two concrete metamaterials **10A**, **10B** exhibited compressibility far beyond conventional concrete. Particularly, the mean values of both concrete metamaterials **10A**, **10B** fell in the vicinity of silicone rubber, which possesses an approximate bulk modulus of 2 GPa. Both concrete metamaterials **10A**, **10B** exhibit compressibility over a factor of 1000 times that of silicone rubber. Conventionally, the properties and behaviors of both materials are exactly the opposite. Concrete exhibits extremely high relative stiffness (high modulus, high density) whereas rubber has close to no relative stiffness (low modulus, low density). In fact, the present disclosure below describes how rubber is commonly used for damping at the base of concrete structures as relative stiffness may work for bearing high loads, but consequentially means the material has close to no strain energy. Yet the concrete metamaterials **10A**, **10B** have effectively reversed the material properties of concrete and endowed rubber like behavior. The material itself has not changed, but the unique reinforcement design of the concrete metamaterials **10A**, **10B** creates an overall composite with unique capabilities.

Calculating the Stiffness

[00058] A concern that would be immediately cited with compressive concrete is a massive sacrifice in stiffness to inversely increase the compressibility of the material. Following up from the discussion of the previous paragraph, achieving high compressibility involves the loss of relative stiffness. Aside from the equation cited in the previous paragraph the bulk modulus can also expressed as $K = \frac{E}{3(1-2v)}$, where E and v are the Elastic Modulus and Poisson's Ratio of the material, respectively [14]. Based on this equation, an ultra-compressive material will either have a low modulus or exhibit large lateral deformations in compression (large Poisson's Ratio). As stiffness is the material resistance to deformation, it seems inherently impossible for a material to be both stiff and compressible. As set forth below, the concrete metamaterials **10A**, **10B** of the present disclosure still maintains high stiffness that accompanies the low bulk modulus calculated above. The fundamental way to assess the stiffness of each concrete metamaterial **10A**, **10B** under compression is to consider the vertical deflection (δ) under the applied load (P). Given the magnitude of the compressive load and vertical displacement by the Instron, the stiffness of each

concrete metamaterial **10A**, **10B** material could be calculated for both cyclic and ultimate compression tests. The stiffness values were plotted against time to get a visual understanding of how the stiffness of each concrete metamaterial **10A**, **10B** changed for each cycle and stage of compression. For cyclic compression, the stiffness values were relatively unstable. **Figure 5** visualizes the wide fluctuation of stiffness between different stages cyclic compression. The stiffness decreases after the first cycle and it takes several cycles for the peak stiffness values to stabilize. This error is directly correlated to the instability in the loading applied by the Instron explained above.

[00059] One key observation from these cyclic stiffness charts and by observing the behaviors of the concrete metamaterials **10A**, **10B** during testing is the startling similarity to a stiff spring. This conceptual understanding initiated the idea for ultimate compression in the second trial of testing. Doing so provided clearer indication of the deformation resistance of each concrete metamaterial **10A**, **10B**. Following a similar procedure to cyclic compression, both concrete metamaterials **10A**, **10B** were tested in different ultimate compression stages applying larger vertical deformation for each successive stage. As shown in **Table 5**, the 3×3 concrete metamaterial **10A** achieved 15 mm, 17.5 mm, and 20 mm of compression for Stages 1, 2, and 3, respectively. The 5× concrete metamaterial **10B** achieved 12.5 mm, 15 mm, 17.5 mm, and 20 mm of compression for Stages 1, 2, 3, and 4, respectively (**Table 5**).

Table 5. Expanded ultimate compression stages for concrete metamaterials **10A**, **10B**.

	Stage	Initial Height (mm)	Final Height (mm)	Initial Volume (mm^3)	Final Volume (mm^3)
3×3 Metamaterial	Stage 1	150	134.98	3,375,000	3,037,051
	Stage 2		132.48		2,980,762
	Stage 3		129.98		2,924,465
5×5 Metamaterial	Stage 1	150	137.48	3,375,000	3,093,337
	Stage 2		134.98		3,037,050
	Stage 3		132.48		2,980,730
	Stage 4		129.98		2,924,451

[00060] The axial load-deformation curves were obtained for the loading phase of each concrete metamaterial **10A**, **10B**. This is defined by the time interval where the compression loading is applied to the moment when the load is released. **Figure 6** shows the obtained P-δ curves.

[00061] Hooke's Law stipulates the stiffness of a material marks the transition from elastic to deformed behavior. During elastic behavior, the deformation curve is linear indicating the rise in vertical displacement of the concrete metamaterial **10A**, **10B** is directly proportional to the rise in compression applied by the Instron device. Once elastic behavior is lost, there is a brief "yield" phase where the auxetic cells **12** of the PolyFlex completely closed and the concrete layers **14** begin to fully bear the applied compressive load. This essentially starts a new deformation curve for the concrete constituency. As the stiffness of the concrete metamaterial **10A**, **10B** is desired, this secondary curve will not be evaluated any further. Returning to the elastic zone of the deformation curves, the transition points are delineated at 5 mm, and 6 mm of vertical displacement for the 3×3 concrete metamaterial **10A** and 5×5 concrete metamaterial **10B**, respectively. Given the load magnitude for each stage of ultimate compression at this transitional position, the stiffness in N/mm was computed. The average of these computations was taken to provide a cumulative estimate of the stiffness for both concrete metamaterials **10A**, **10B**. The results are shown in **Table 6**.

Table 6. Computed stiffness values for the ultimate compression testing of each concrete metamaterial **10A**, **10B**.

	Stage	**Load at Transition (N)**	**Stiffness (N/mm)**
3×3 Metamaterial	Stage 1	1952	390
	Stage 2	1868	374
	Stage 3	1803	360
	Mean	1874	382
5×5 Metamaterial	Stage 1	3794	632
	Stage 2	3507	584
	Stage 3	3373	561
	Stage 4	2890	481
	Mean	3391	565

Strain Analysis

[00062] For the duration of both trials of cyclic testing, the strains were recorded via the two gauges **30** placed at the central concrete layer **19** of each of the concrete metamaterials **10A**, **10B**. It was of interest to understand the strain in the concrete part **14**, **19** of each concrete metamaterial **10A**, **10B** to verify the load reduction provided by the PolyFlex reinforcement **12**. Also given the intricate geometry of the concrete layers **14**, **19**, it was desired to pinpoint the areas of geometry bound to undergo the largest stress. Mapping out the strain distribution will contribute at future design modifications aimed at curtailing unusually high stresses brought upon by the original design. The middle layer **19** of each concrete metamaterial **10A**, **10B** was chosen as that layer experienced full vertical displacement and was equidistant from the interfacing surfaces **16**, **18** between each concrete metamaterial **10A**, **10B** and the Instron device. The maximum and minimum strains were obtained, and the difference taken to assess the change in strain between compression and release. The results for the 3×3 concrete metamaterial **10A** and 5×5 concrete metamaterial **10B** are shown in Tables 7 and 8, respectively. The strain sensor **30** located at the center of concrete layer **19** of the 5×5 concrete metamaterial **10B** failed to produce viable readings leaving only the strain measurements at the side of layer **19**.

Table 7. Measured strain values for the cyclic compression testing of the 3×3 concrete metamaterial **10A**.

3×3 Metamaterial Strains	Central Strain (με/ε)			Side Strain (με/ε)		
	Maximum	Minimum	Difference	Maximum	Minimum	Difference
Stage 1 – Trial 1	-4.63E-06	-2.49E-05	2.02E-05	-1 01E-06	-3.56E-05	3.46E-05
Stage 1 – Trial 2	4.67E-06	-1.46E-05	1.93E-05	1.31E-05	-3.02E-05	4.34E-05
Stage 2 – Trial 1	6 05E-06	-2 88E-05	3.49E-05	1.19E-06	-4.52E-05	4.64E-05
Stage 2 – Trial 2	-7.24E-06	-2.69E-05	1.97E-05	7 13E-06	-3.82E-05	4.54E-05
Stage 3 – Trial 1	-1 38E-05	-3 14E-05	1.76E-05	3.54E-06	-4.12E-05	4.48E-05
Stage 3 – Trial 2	4.08E-06	-2.11E-05	2.52E-05	6.05E-06	-4 40E-05	5 01E-05
Mean	-2.99E-06	-2.46E-05	2 28E-05	5.00E-06	-3.91E-05	4.41E-05

Table 8. Measured strain values for the cyclic compression testing of the 5×5 concrete metamaterial **10B**.

5×5 Metamaterial Strains	Side Strain (με/ε)		
	Maximum	Minimum	Difference
Stage 1	-7.30E-06	-2.02E-05	1.29E-05
Stage 2	-9.65E-06	-2 76E-05	1.79E-05
Stage 3	-1.39E-05	-3.00E-05	1.61E-05

Stage 4	-2.05E-05	-3.84E-05	1.79E-05
Mean	-1.28E-05	-2.90E-05	1.62E-05

[00063] In addition to compiling the extreme strains in the data, the readings were plotted against time to assess if the readings aligned with the mechanics of cyclic compression (**Figure 7**). The measurements showed the expected variation inherent to cyclic compression.

[00064] The strains at the center layer **19** for the 3×3 concrete metamaterial **10A** showed the cleanest behavior where the peaks were centered around approximately -17.5 με and uniformly increased between each successive stage. Note that there was a much larger increase in strain between Stages 1 and 2 compared to Stages 2 and 3 at the center of the layer **19**. This indicates that the auxetic cells **12** have essentially closed and the concrete **14** is bearing the entirety of the load. The minimal change in strain is a testament to concrete strength in compression. Observing the changes on the side strain graph, the sensor readings were centered around -15 με for the Stage 1 of compression, but suddenly jumps to -5 με at Stage 2 before falling slightly to -7.5 με at Stage 3. As the side strain gauge was located at the end of a curved portion of the layer this behavior is an effect of concrete arranged in a complicated geometry. At the height of compression for each stage, the layer **19** would experience a positive moment and the ends of the layer **19** would slightly rotate. This explains the sudden transition from negative to positive strains as the compression distance increased. Then from Stages 2 to 3, the decrease in strain may be due to further rotation of the layer shifting the stresses farther to the sides of the layer. This goes hand in hand with the minimal increase in strain at the center of the layer **19** as well.

[00065] The strain measurements at the side of layer **19** of the 5×5 concrete metamaterial **10B** showed an opposite trend to the 3×3 concrete metamaterial **10A**, which saw greater negative strains corresponding to increased compression distance. This is simply because the 5×5 concrete metamaterial **10B** was compressed in inverse manner to the 3×3 concrete metamaterial **10A**, which switched the sign on the strain measurements. The strain measurements at Stages 1 and two were aligned at the peaks, yet the strain cycles at Stage 2 were roughly twice the size. The cycles remained the same size from Stages 2 through 4 but shifted downward 7.5 με between Stage 2 and 3, and 5 με between Stages 3 and 4. Given that the change is vertical displacement is the same

between these stages (2.5mm) the slight decrease of the change in strain can be attributed to what was observed for the 3×3 concrete metamaterial **10A**. The compactness and higher deformation resistance of the 5×5 concrete metamaterial **10B** did not make the flow of forces as apparent, but as the vertical compression distance is increased the load seems to shift towards the outside of the specimen thereby decreasing the strain values exhibited at the center of the layer **19**. **Figure 8** shows the strain readings obtained for the multiple stages of ultimate compression testing. Significant damage was incurred by the concrete layers **14** during this phase of testing since the displacement was past the spatial limit of the PolyFlex reinforcement **12**.

[00066] For the 3×3 concrete metamaterial **10A**, the strain values peaked at the side and center of the layer **19** at approximately 12.5 seconds. This did not correspond to when the concrete metamaterial **10A** was released during ultimate compression testing at 20 seconds. This is most likely because the loading did not increase after 10 seconds, resulting in a sharp peak and decrease in the strain values. Between stages the strain magnitude did not vary significantly and exhibited an increasing negative trend with the peak occurring sooner for each subsequent stage. The position of the strain gauges **30** was highly coordinated for this phase of testing with the strain readings off center reporting peak values roughly 2 με lower than the measurements at the center of the layer **19** for each stage. From cyclic compression, it was observed the sides experienced a positive moment in the latter stages of testing, but this did not occur during ultimate compression. After the auxetic cells **12** of the PolyFlex closed, the side rotation stopped, and the concrete layers **14** were fixated in pure compression. Therefore, the strain measurements at this phase of testing showed higher magnitudes and overall consistency. The strain measurements for the 5×5 concrete metamaterial **10B** were much more erroneous and did not shown any viable or consistent trends compared to the 3×3 concrete metamaterial **10A**. Since the measurements at the center of the layer **19** were discarded altogether for similar reasons, the strain readings for this phase of testing are not shown.

Finite Element Modelling

[00067] To further analyze the comprehensive geometry, the designs of each concrete metamaterial **10A**, **10B** was uploaded to Abaqus CAE to generate a finite element model (FEM)

that could simulate all the actual testing performed on the metamaterials. The complexity of both concrete metamaterials **10A**, **10B** generated a robust FEM that would have taken massive computational power to achieve convergence. Therefore, the cross-sectional depth was removed and a 2D version of each concrete metamaterial **10A**, **10B** was used to simplify the FEM. The material properties of cement paste **14** and PolyFlex structure **12** were inserted and applied accordingly to each component of the FEM (**Table 9**).

Table 9 - Material properties used for FE analysis.

Material	Density (kg/m3)	Youngs Modulus (Pa)	Poisson's Ratio
PolyFlex (21.5 °C)[15]	1205	9,400,000	N/A
Cement Paste[16]	1600	450,000,000	0.28

[00068] To begin, three steps were created as a placeholder for each stage of cyclic compression. Boundary conditions were applied to fix all degrees of freedom on the bottom surface and apply a vertical displacement equivalent to the maximum for each stage. The 5×5 concrete metamaterial **10B** possessed more intricacies than the 3×3 concrete metamaterial **10A** and required a much finer mesh to adequately encapsulate the geometry. Once a compression stage was simulated, a stress distribution was computed by Abaqus for the deformed state. Certain elements were able to be selected for the strain outputs, and the elements that coincided with the locations of the strain gauges during testing were chosen. The FE simulation results are shown in **Figure 9**.

Damage Resistance

[00069] During both phases of testing, several cracks were observed in the concrete layers **14**. Beginning in cyclic compression, these cracks achieved full vertical progression and parts of the cement paste layer were separated. **Figure 10** shows the damage progression through a cycle of compression. Despite damage in multiple layers, the material functionality and behaviors were not affected whatsoever. The bonding between the cement paste **14** and the polymer structure **12** was strong enough to maintain the stiffness and stability of each concrete metamaterial **10A**, **10B**. This further accentuates the potential high-level damping capabilities of the concrete metamaterials **10A**, **10B**. Here, the present disclosure presents a proof-of-concept compressible concrete metamaterials **10A**, **10B** using a simple cement mixture that has not yet been optimized

for damage resistance. There are certainly multiple solutions to improve the cement/concrete mixture properties (e.g. adding fibers) for a better damage resistance.

Future Work and Applications

[00070] The present disclosure has shown how preferred concrete metamaterials **10A**, **10B** can provide model extreme compressibility. Furthermore, any fault that occurs in the cement paste layers **14** do not impact the overall functionality of the concrete metamaterials **10A**, **10B**. As such, the concrete metamaterials **10A**, **10B** could very well be used in applications for which concrete has not previously been considered and bolster concrete performance in applications for which it is already considered efficient.

Redefining the Concrete Beam

[00071] A cubic model of the concrete metamaterials **10A**, **10B** was chosen to obtain base material properties for the innovative material geometry and composite constituency of the present disclosure. By no means is this the final construction form for this concept. **Figure 11** illustrates larger specimen that better illustrates the future design goals for the composite concrete metamaterials of the present disclosure. This could be considered the very first concrete "beam-column" as it will have the ability to exhibit high resistance to compression and lateral forces. In concrete construction, concrete columns have the tendency to be overdesigned due to fear of unpredictable loads, which expose the weaknesses of concrete in tension and fatigue. As previously stated, the polymer reinforcement acts as a surface protect to prevent initial flaws on the concrete surface, preventing seepage and subsequent freeze-thaw effects in areas subject to seasonal changes. Also, the polymer reinforcement **12** was observed to have bonded so well with the cement paste **14**, that full crack progression did not induce any observable loss in stiffness. The very weaknesses that engineers choose to overdesign concrete buildings for are eliminated through the innovations incorporated into the concrete metamaterials of the present disclosure, including concrete metamaterials **10A**, **10B**. The concrete metamaterials of the present disclosure may also supersede steel reinforcement of concrete in the long term as the polymer or PolyFlex structure **12** is an inert material and will not corrode or degrade over the serviceable lifetime of the structure.

Design costs can be considerably decreased considering the all-around efficiency of the concrete metamaterials of the present disclosure.

[00072] **FIG. 11.** shows a preferred unit slab concept design for the 3×3 metamaterial polymer formwork **10A** of the present disclosure with potential applications of the proposed metamaterial concrete of: (a) a high energy absorbing engineered materials arresting system **40**, (b) metamaterial concrete base isolation system **50**, (c) A shock absorbent bike lane pavement **60**.

Damping Capabilities

[00073] There is a stunning multitude of technologies to combat seismic forces on rigid structures, yet an ideal solution has yet to be found that combines low cost with high seismic resilience. The most popular solution is damping applications, to dissipate the energy of ground movement during an earthquake. Technically speaking these dampers are called *base isolation systems*, which serve to decouple a super structure from the ground and greatly reduce the effect of seismic loads [15]. These are found to greatly reduce building acceleration and inter-story drift of the superstructure. Elastomers are sought for this application as they exhibit high damping properties and can undergo nonlinear deformations while maintaining elastic behavior. As the relative stiffness of elastomers are so low, they are layered with thin metal plates as to maintain high damping characteristics under the sheer weight of the super structure. The primary setback of this method is the difficulty achieving the proper vibration frequency equivalent to that of a seismic event. Fundamentally speaking, a multi-story concrete structure requires damping for multiple degrees of freedom. Leaving a large unbraced length in a concrete girder or columns guarantees fatigue no matter how much you reduce vibrations at the base of the super structure. The concrete metamaterials of the present disclosure as described above can be both retrofitted to any concrete column size in a superstructure or precast and delivered in different concrete forms, notably columns or girders. The compressibility and stiffness of the concrete metamaterials of the present disclosure can be tuned based on the number of auxetic cells **12** included in the design. With further research and testing, this design can be matched to any known building frequency. Endowing concrete girders with damping capabilities will further improve the structural resistance of concrete to ground acceleration and inter-story drift. Rather than merely focusing on the interface

between the superstructure and the subgrade, the concrete metamaterials of the present disclosure will enable a holistic approach to damping in concrete structures. Additionally, the concrete metamaterials of the present disclosure may also pose as an ideal solution for other types of structures beyond concrete. The first common concrete-only structures that struggle in terms of design longevity are parking garages. Concrete is the choice material as the dominating load to consider in the design of parking garages is compression. Though concrete is the correct choice for this application, there are other design variables in a parking garage that also work against conventional concrete. The first major issue is a phenomenon known as *spalling*. As previously mentioned, the brittleness of concrete tends to produce a lot of surface flaws, and it is bad news when moisture penetrates these surface flaws. The water that enters the surface can cause the flaw to progress deeper into the slab and increase the surface area of the flaw, allowing even more moisture to penetrate the concrete. It is a vicious cycle that can cost a lot in repairs as it may happen frequently in parking garages in areas of high moisture or precipitation.

[00074] Another factor to consider is vibration, which can be severe in peak traffic hours. To reiterate, the brittle nature of concrete means that the ability of this material to dissipate energy is close to nothing. That means the concrete columns in parking garages must be large as to not produce a lot of flaws in response to heavy vibration. The concrete metamaterials of the present disclosure are the perfect solution for columns or slabs in parking garages due to the polymer cover and extreme compressibility. The advantages of the polymer reinforcement **12** of the concrete metamaterials **10A**, **10B** were mentioned in the previous section, so consider how the compressibility completely changes how an engineer would approach this design. The design geometry endows the concrete metamaterials **10A**, **10B** of the present disclosure with the ability to dissipate vibration energy without producing any surface flaws in the concrete and it is now known that the concrete metamaterials **10A**, **10B** will still function at a high level with the presence of surface flaws. When considering the issues with concrete parking garages, the concrete metamaterials **10A**, **10B** could pose as a viable alternative for sidewalks, outdoor stairways, and Portland cement concrete (PCC) pavements. With these applications in particular, the advantage of using the concrete metamaterials **10A**, **10B** of the present disclosure is that the design does not require coarse aggregates in the concrete mixture. With some added strength, the concrete metamaterials **10A**, **10B** of the present disclosure would be useful for constructing sidewalks and

roadways capable of energy dissipation from the passing of cars or human foot traffic. The responsivity of the concrete metamaterials of the present disclosure to compressive force may ensure a much longer serviceable lifetime for the sidewalk and/or roadway compared to what is used presently, further saving construction costs in the form of road repairs.

Conclusion

[00075] The present disclosure is directed to design a new generation of concrete metamaterials with extreme compressibility and mechanical tunability. The concrete metamaterials of the present disclosure incorporate the fusion of snapping metamaterials and concrete design concepts. Integrating the concrete mixture **14** with auxetic polymer structures **12** with snap-through buckling behavior resulted in the concrete metamaterials **10A**, **10B** of the present disclosure having new functionalities. The developed proof-of-concept concrete metamaterials **10A**, **10B** were experimentally tested to verify the efficient of the proposed concept. The results were in a reasonable agreement with the numerical simulations. The abilities of the concrete metamaterials **10A**, **10B** could potentially revolutionize concrete construction as it supplements the inherent weaknesses of concrete in fatigue applications. The overall design of the concrete metamaterials **10A**, **10B** instead should be recognized as a concrete reinforced polymer as the polymeric auxetic metamaterial structure is what truly incorporates the compressible property into concrete. The composite constituency of the concrete metamaterials **10A**, **10B** showed levels of compressibility greater than cork, while maintaining a high level of stiffness. The compressibility of concrete metamaterials of the present disclosure provides for a ductile concrete, with a significantly higher flexural capacity and ability to absorb vibration without incurring any flaws. Preferably, more focus will be place on mechanical tunability of the concrete metamaterials of the present disclosure via parameters such as the number of auxetic cells, the polymer material and the composition of the concrete mixture. Additionally, future work preferably will focus on different empirical forms of the concrete metamaterials of the present disclosure, such as beams and slabs, which are likely to be the most widely used application for the concrete metamaterials of the present disclosure.

References

[00076] [1] Y. Fu , X. Wang , L. Wang , Y. Li. Hindawi Advances in Materials Science and Engineering Volume 2020, Article ID 6153602, 25 pages.

[00077] [2] Wang, L., Jiang, H., Li, Z. *et al.* Mechanical behaviors of 3D printed lightweight concrete structure with hollow section. *Archiv.Civ.Mech.Eng* 20, 16 (2020).

[00078] [3] Brian Salazar, Parham Aghdasi, Ian D. Williams, Claudia P. Ostertag, Hayden K. Taylor, Polymer lattice-reinforcement for enhancing ductility of concrete, Materials & Design, Volume 196, 2020, 109184, ISSN 0264-1275,

[00079] [4] Lijing Kang, Wei Fan, Bin Liu, Yanzhi Liu, Numerically efficient analysis of concrete-filled steel tubular columns under lateral impact loading, Journal of Constructional Steel Research, Volume 179, 2021, 106564, ISSN 0143-974X,

[00080] [5] Zhijie Huang, Wensu Chen, Hong Hao, Zuyu Chen, Thong M. Pham, Tung T. Tran, Mohamed Elchalakani, Shear behaviour of ambient cured geopolymer concrete beams reinforced with BFRP bars under static and impact loads, Engineering Structures, Volume 231, 2021, 111730, ISSN 0141-0296,

[00081] [6] Jiao P., Alavi A.H., "Artificial intelligence-enabled smart mechanical metamaterials: advent and future trends", International Materials Reviews, 1-29, 2020.

[00082] [7] Zadpoor A. A., Mechanical metamaterials. Mater. Horiz. 3, 371-381 (2016).

[00083] [8] Barri K., Zhang Q., Jiao P., Chen J., Wang ZL., Alavi A.H., "Multifunctional meta-tribomaterial nanogenerators for energy harvesting and active sensing", Nano Energy, Article 106074, 2021.

[00084] [9] Xianglong Yu, Ji Zhou, Haiyi Liang, Zhengyi Jiang, Lingling Wu, Mechanical metamaterials associated with stiffness, rigidity and compressibility: A brief review, Progress in Materials Science, Volume 94, 2018, Pages 114-173, ISSN 0079-6425,.

[00085] [10] Hang Yang, Li Ma, Multi-stable mechanical metamaterials with shape-reconFigureuration and zero Poisson's ratio, Materials & Design, Volume 152, 2018, Pages 181-190, ISSN 0264-1275, https://doi.org/10.1016/j.matdes.2018.04.064.

[00086] [11] Huang Gu, Zuo Zhong e, Compressive behaviours and failure modes of concrete cylinders reinforced by glass fabric, Materials & Design, Volume 27, Issue 7, 2006, Pages 601-604, ISSN 0261-3069.

[00087] [12] Chen, E., Berrocal, C.G., Löfgren, I. *et al.* Correlation between concrete cracks and corrosion characteristics of steel reinforcement in pre-cracked plain and fibre-reinforced concrete beams. *Mater Struct* 53, 33 (2020).

[00088] [13] ACI 318, Building Code Requirements for Structural Concrete (ACI 318-05) and Commentary (ACI 318R-05), ACI Committee 318, American Concrete Institute, Farmington Hills, MI, 2005

[00089] [14] Courtney, Thomas H. *Mechanical Behavior of Materials*. McGraw Hill Education (India), 2013.

[00090] [15] SteenhuisC., M. "Resistance and Stiffness of Concrete in Compression and Base Plate in Bending." (2005).

[00091] All patents, patent applications, provisional applications, and publications referred to or cited herein are incorporated by reference in their entirety for all purposes.

[00092] It should be understood that the examples and embodiments described herein are for illustrative purposes only and that various modifications or changes in light thereof will be suggested to persons skilled in the art and are to be included within the spirit and purview of this application and the scope of the appended claims.

What is claimed is:

1. A metamaterial, comprising:

an auxetic lattice structure with snap-through buckling behavior comprising a plurality of rows; wherein the lattice defines a holey arrangement array; and

cement, concrete or any other brittle materials disposed in the auxetic lattice structure.

2. The metamaterial of claim **1**, wherein the auxetic lattice structure comprises a polymer.

3. The metamaterial of claim **1**, wherein the auxetic lattice structure comprises a thermoplastic polyurethane.

4. The metamaterial of claim **1**, wherein each row of the auxetic lattice structure defines a channel or conduit in which the cement, concrete or any other brittle materials are disposed.

5. The metamaterial of claim **4**, wherein each channel or conduit has an open side or end for receiving the cement, concrete or any other brittle materials.

6. The metamaterial of claim **5**, wherein each row defines one or more curved sections.

7. The metamaterial of claim **5**, wherein each row defines a plurality of curved sections.

8. The metamaterial of claim **1**, wherein the cement or concrete comprises a mixture of Type I/II Portland cement and water.

9. The metamaterial of claim **8**, wherein a maximum water to cement ratio of 0.45.

10. The metamaterial of claim **1**, wherein the compressibility of the metamaterial is varied by varying the Young's Modulus and/or Poisson's Ratio of the auxetic lattice structure and/or the cement or concrete.

11. The metamaterial of claim **1**, wherein the metamaterial does not exhibit transverse strain under compression.

12. The concrete metamaterial of claim **1**, wherein the holey arrangement array comprises a 3x3 array or a 5x5 array.

13. The concrete metamaterial of claim **1**, further comprising one or more level or planar surfaces.

14. The metamaterial of claim **1**, wherein the metamaterial undergoes pattern transformation under compression to allow vertical displacement of the metamaterial, equivalent to a dimension of the holey arrangement array, from a default position and when compression of the metamaterial is discontinued, the metamaterial undergoes another pattern transformation and returns to the default position.

15. The metamaterial of claim **1**, wherein the auxetic lattice structure comprises a material with a low Young's modulus (E) and high Poisson's ratio (v).

16. A metamaterial, comprising:

a flex design comprising a concrete or cement material disposed in an auxetic structure with snap-through buckling behavior; and

a cement, concrete or any other brittle materials disposed in the auxetic lattice structure.

17. The metamaterial of claim **16**, wherein the auxetic structure has a plurality of rows and defines a holey arrangement array.

18. The metamaterial of claim **16**, wherein the auxetic structure comprises a polymer or a thermoplastic polyurethane.

19. The metamaterial of claim **17**, wherein each row of the auxetic structure defines a channel or conduit in which the cement, concrete or any other brittle materials are disposed.

20. The metamaterial of claim **17**, wherein each row defines one or more curved sections.

21. The metamaterial of claim **16**, wherein the cement or concrete comprises a mixture of Type I/II Portland cement and water.

22. The metamaterial of claim **21**, wherein a maximum water to cement ratio of 0.45.

23. The metamaterial of claim **16**, wherein the compressibility of the metamaterial is varied by varying the Young's Modulus and/or Poisson's Ratio of the auxetic lattice structure and/or the cement or concrete.

24. The metamaterial of claim **16**, wherein the metamaterial does not exhibit transverse strain under compression.

25. The metamaterial of claim **17**, wherein the holey arrangement array comprises a 3x3 array or a 5x5 array.

26. The metamaterial of claim **16**, further comprising one or more level or planar surfaces.

27. The metamaterial of claim **17**, wherein the metamaterial undergoes pattern transformation under compression to allow vertical displacement of the metamaterial, equivalent to a dimension of the holey arrangement array, from a default position and when compression of the metamaterial is discontinued, the metamaterial undergoes another pattern transformation and returns to the default position.

28. The metamaterial of claim **16**, wherein the auxetic structure comprises a material with a low Young's modulus (E) and high Poisson's ratio (v).

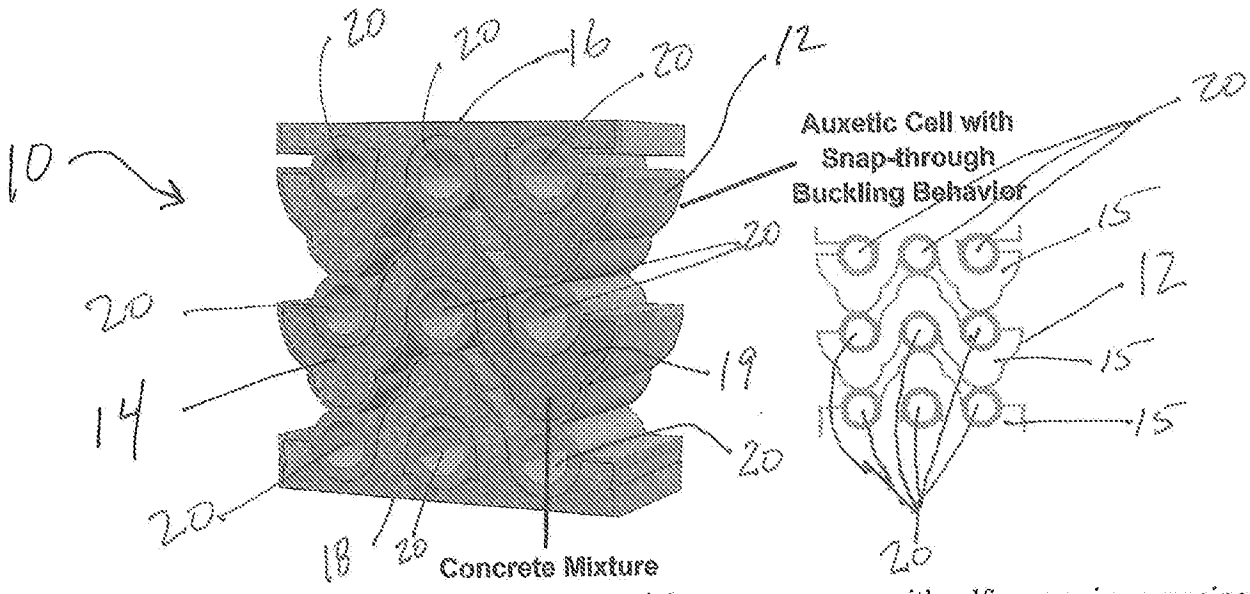

Figure 1. Vision for a composite metamaterial concrete system with self-recovering snapping segments.

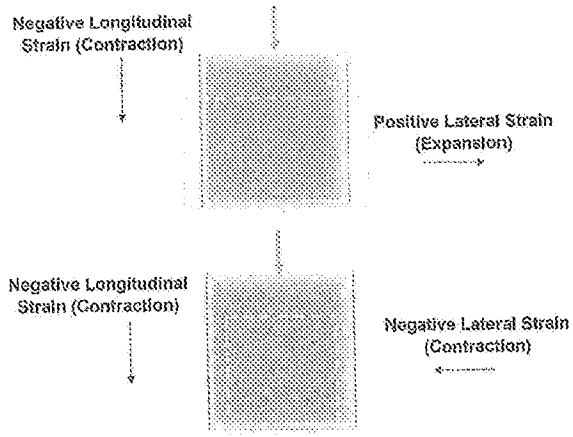

Figure 2. Unit material under compression exhibiting positive Poisson's ratio (top) and negative Poisson's ratio (bottom).

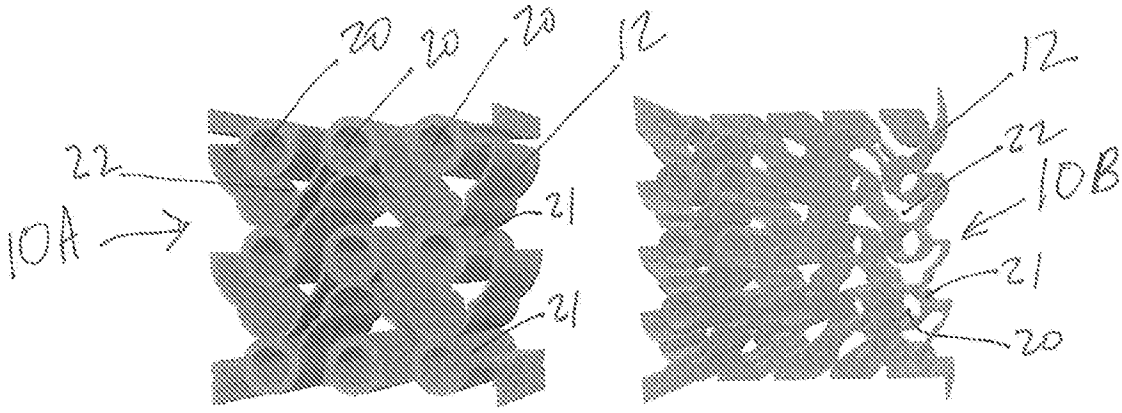

(a) (b)

Figure 3. Metamaterial concrete polymeric lattices comprised of (a) 3×3 unit cells, (b) 5×5 unit cells.

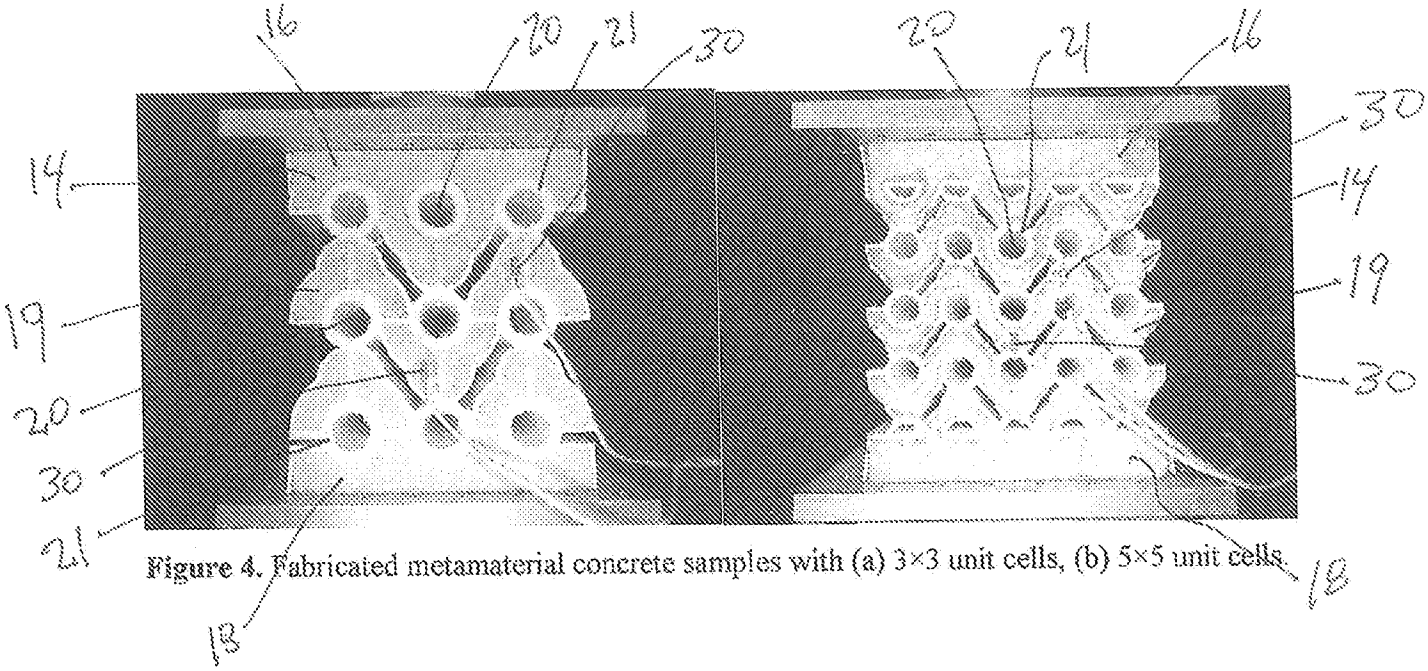

Figure 4. Fabricated metamaterial concrete samples with (a) 3×3 unit cells, (b) 5×5 unit cells.

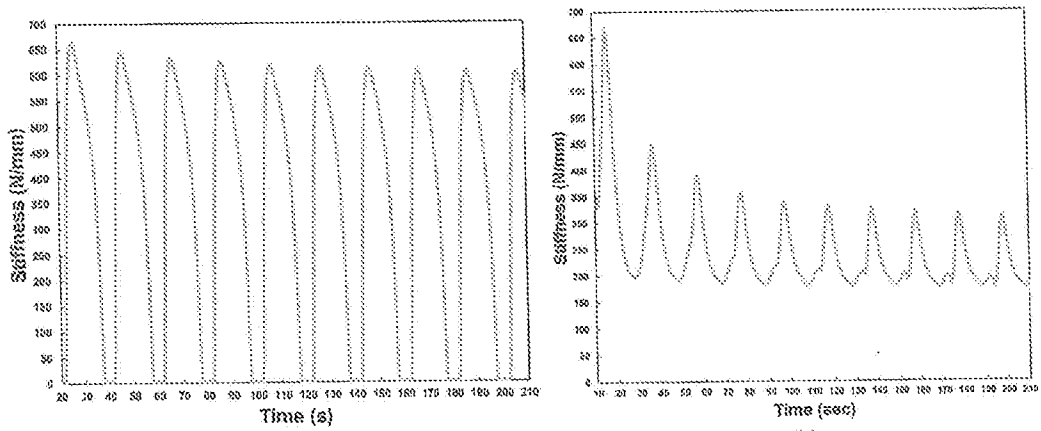

(a) (b)

Figure 5. Stiffness versus time for tests at Stage 1 compression: (a) 4 mm vertical displacement, (b) 5 mm vertical displacement.

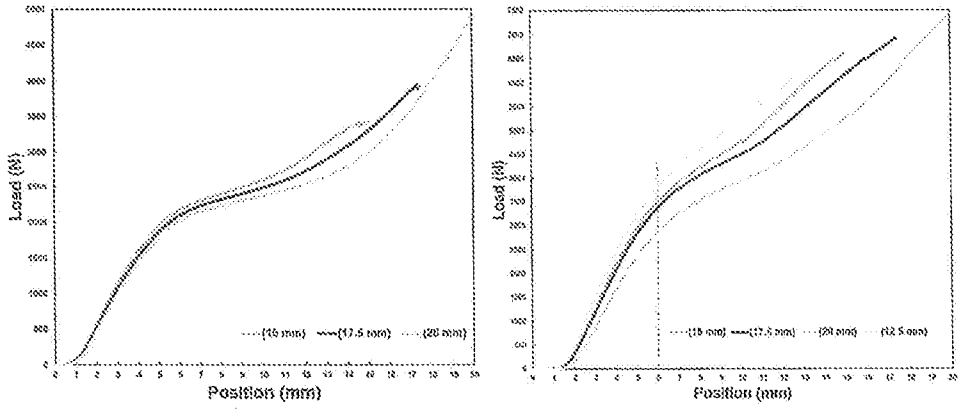

Figure 6. P-δ curves illustrated for (a) 3×3 sample, (b) and 5×5 sample.

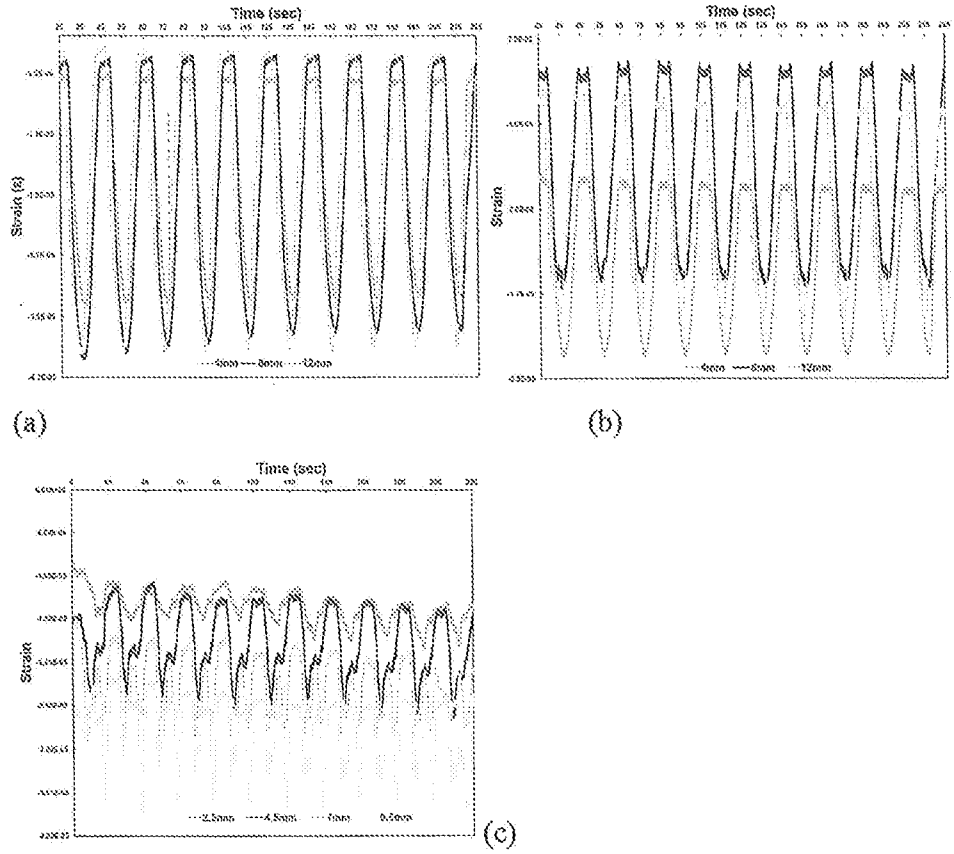

Figure 7. Cyclic compression strain readings plotted against time for (a) 3×3 design side gauge, (b), 3×3 design center gauge (c) 5×5 design side gauge.

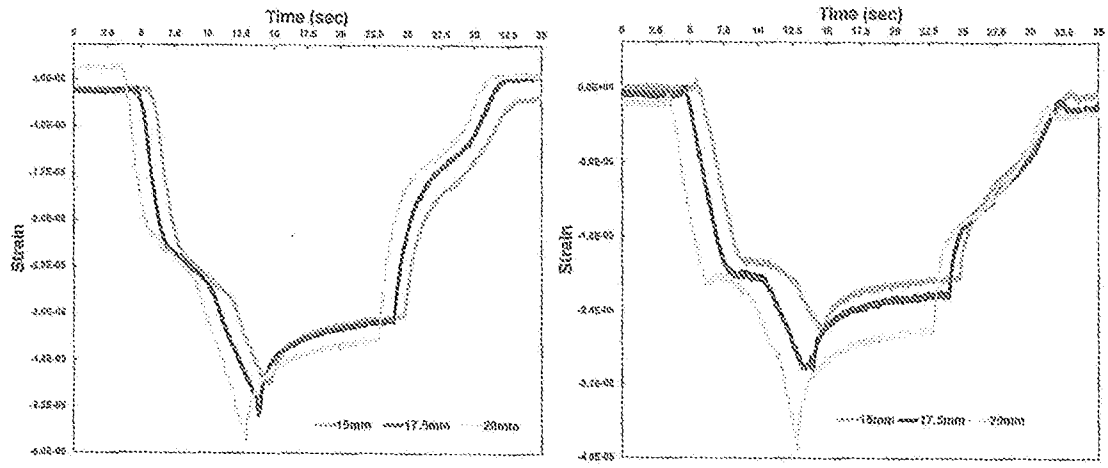

(a) (b)

Figure 8. Ultimate compression strain readings plotted against time for (a) 3×3 design side gauge, (b) 3×3 design center gauge.

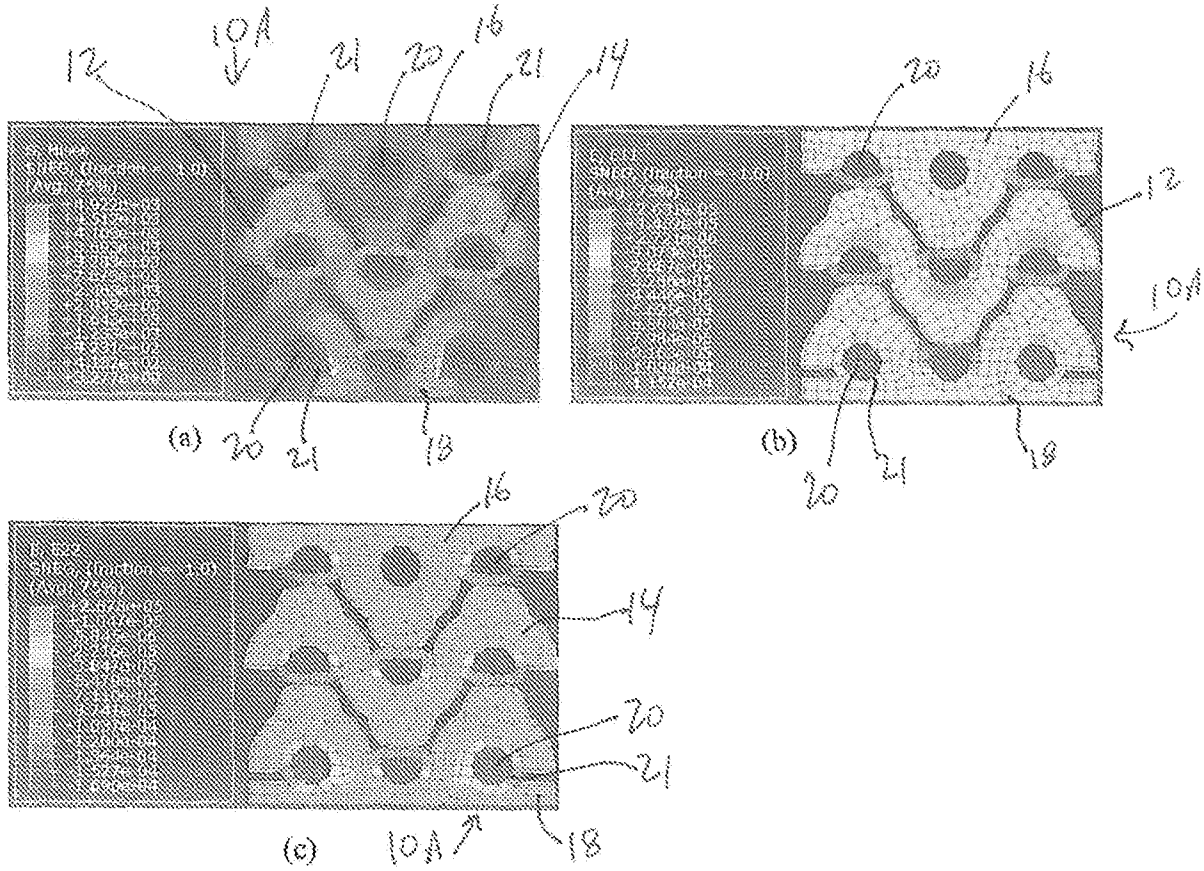

Figure 9. FE simulation results: (a) Mises stresses, (b) Transverse strains, (c) Longitudinal strains.

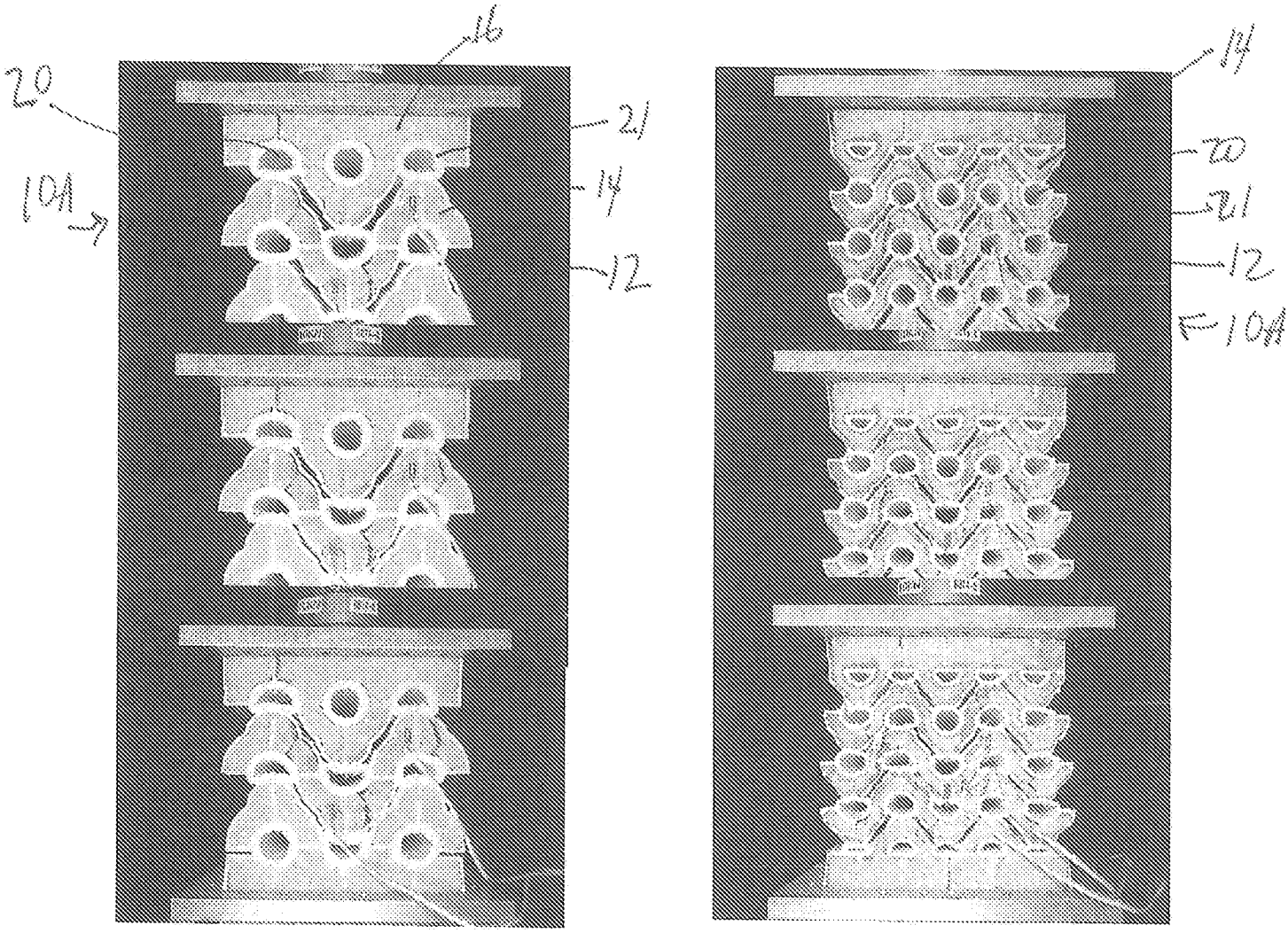

Figure 10. Illustration of damage progression through a cycle of compression for: (a) 3×3 designs, (b) 5×5 designs.

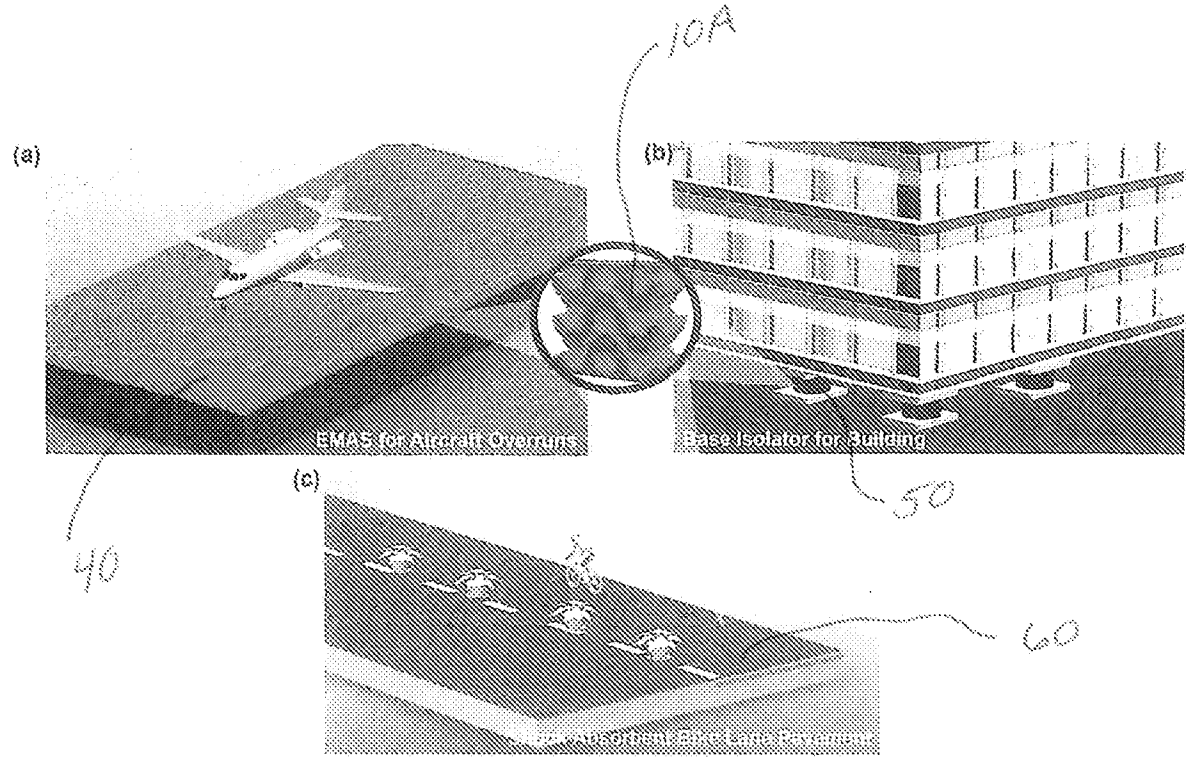

Figure 11. Unit slab concept design for the 3×3 metamaterial polymer formwork. Potential applications of the proposed metamaterial concrete: (a) A high energy absorbing engineered materials arresting system, (b) Metamaterial concrete base isolation system, (c) A shock absorbent bike lane pavement.

INTERNATIONAL SEARCH REPORT

International application No.
PCT/US 22/44016

A. CLASSIFICATION OF SUBJECT MATTER

IPC - INV. E04C 5/00, B28B 23/00 (2022.01)
ADD. B32B 13/04, C04B 7/02 (2022.01)

CPC - INV. E04C 5/00, B28B 23/00, B28B 1/008
ADD. B32B 13/04, C04B 7/02, C04B 2201/50, C04B 38/0006

According to International Patent Classification (IPC) or to both national classification and IPC

B. FIELDS SEARCHED

Minimum documentation searched (classification system followed by classification symbols)
See Search History document

Documentation searched other than minimum documentation to the extent that such documents are included in the fields searched
See Search History document

Electronic data base consulted during the international search (name of data base and, where practicable, search terms used)
See Search History document

C. DOCUMENTS CONSIDERED TO BE RELEVANT

Category*	Citation of document, with indication, where appropriate, of the relevant passages	Relevant to claim No.
A	Rosewitz et al. "Bioinspired design of architected cement-polymer composites" Cement and Concrete Composites, Vol 96 (17 December 2018): pages 252-265; entire document, but especially: abstract, page 253 col 2 para 1, page 253 col 2 para 4, page 253 col 2 para 4, fig. 1, fig. 2	1-28
A	US 2016/0025344 A1 (President and Fellows of Harvard College et al.) 28 January 2016 (28.01.2016); entire document, but especially: para [0009], para [0037], fig. 1b, fig. 1c, fig. 1d	1-28
A	US 2017/0362414 A1 (The Royal Institution for the Advancement of Learning/McGill University) 21 December 2017 (21.12.2017); entire document, but especially: para [0007], para [0059], fig. 2a-2f, fig. 3a-3f	1-28
X, P	US 2022/0209686 A1 (University of Pittsburgh - Of the Commonwealth System of Higher Education) 30 June 2022 (30.06.2022); entire document	1-28

☒ Further documents are listed in the continuation of Box C. ☐ See patent family annex.

* Special categories of cited documents:
"A" document defining the general state of the art which is not considered to be of particular relevance
"D" document cited by the applicant in the international application
"E" earlier application or patent but published on or after the international filing date
"L" document which may throw doubts on priority claim(s) or which is cited to establish the publication date of another citation or other special reason (as specified)
"O" document referring to an oral disclosure, use, exhibition or other means
"P" document published prior to the international filing date but later than the priority date claimed
"T" later document published after the international filing date or priority date and not in conflict with the application but cited to understand the principle or theory underlying the invention
"X" document of particular relevance; the claimed invention cannot be considered novel or cannot be considered to involve an inventive step when the document is taken alone
"Y" document of particular relevance; the claimed invention cannot be considered to involve an inventive step when the document is combined with one or more other such documents, such combination being obvious to a person skilled in the art
"&" document member of the same patent family

Date of the actual completion of the international search	Date of mailing of the international search report
28 November 2022	JAN 11 2023
Name and mailing address of the ISA/US Mail Stop PCT, Attn: ISA/US, Commissioner for Patents P.O. Box 1450, Alexandria, Virginia 22313-1450 Facsimile No. 571-273-8300	Authorized officer Kari Rodriquez Telephone No. PCT Helpdesk: 571-272-4300

INTERNATIONAL SEARCH REPORT

International application No.
PCT/US 22/44016

C (Continuation). DOCUMENTS CONSIDERED TO BE RELEVANT

Category*	Citation of document, with indication, where appropriate, of the relevant passages	Relevant to claim No.
X, P	Barri et al. "Super Compressible Multifunctional Metamaterial Concrete" Society of Photo-Optical Instrumentation Engineers (SPIE) (20 April 2022): pages 1-9; entire document	1-28
A	Rafsanjani et al. "Snapping Mechanical Metamaterials under Tension" Advanced Materials (October 2015): pages 1-11; entire document	1, 16
A	US 2011/0240194 A1 (Summers et al.) 06 October 2011 (06.10.2011); entire document	1-28